International Journal of Heat and Mass Transfer 52 (2009) 4573–4583

Contents lists available at ScienceDirect

International Journal of Heat and Mass Transfer

journal homepage: www.elsevier.com/locate/ijhmt

Performance characteristics of a vapor feed passive miniature direct methanol fuel cell

Gregory Jewett, Zhen Guo, Amir Faghri *

Department of Mechanical Engineering, University of Connecticut, 261 Glenbrook Road, Unit 2337, Storrs, CT 06169, United States

ARTICLE INFO

Article history:
Received 2 February 2009
Received in revised form 7 March 2009
Accepted 7 March 2009
Available online 4 May 2009

Keywords:
Direct methanol fuel cell
Passive
Vapor feed

ABSTRACT

In this paper, a new vapor feed fuel delivery system for a passive direct methanol fuel cell (DMFC) is developed and tested. Anode hydrophilic layers, electrical heating power and carbon dioxide release are examined to find their effects on the power density, efficiency and average temperatures of the cell. The hydrophilic layers act as a buffer layer between the vapor chamber and the anode gas diffusion layer (GDL). This layer allows water and methanol to mix, as well as distribute uniformly across the anode surface. Measurement of several parameters such as current, voltage, power, internal resistance, vapor chamber pressure, relative humidity and carbon dioxide concentration are taken. A maximum power density of 33 mW cm^{-2} is achieved as well as 120 h of continuous operation at a constant current of 50 mA cm^{-2} using the vapor feed system. The fuel utilization efficiency during the 120 h test is 34.8% and the energy efficiency is 8.2%.

1. Introduction

Direct methanol fuel cells (DMFCs) are being looked to for portal power sources due to their potential for greater power density, smaller size and weight, shorter recharging (instant) and longer runtimes than batteries [1]. The most significant obstacle in developing DMFCs is methanol crossover, a process in which methanol diffuses through the membrane, reacts at the cathode side and lowers the conversion efficiency. Methanol crossover can be reduced by maintaining a dilute concentration between 2.0 and 3.0 mol kg^{-1} [2,3]. A dilute concentration of methanol and water has poor energy efficiency, therefore storing and delivering pure methanol is favored. Pure methanol can be supplied to the anode of the cell in either a liquid or vapor form and mixed with water at the anode [4].

There are two distinctions for fuel delivery systems: active and passive. Active systems have multiple components that make up the balance of plant, which consist of pumps, blowers and fans. Compared with active systems, passive DMFCs have the advantage of eliminating the external parts and systems by controlling the methanol concentration by passive means, such as phase changes, wicking and diffusion.

Scott et al. [5] compared both liquid and vapor feed DMFCs for active DMFCs. In these systems, a pump feeds aqueous methanol solution to the anode of the cell and compressed oxygen is fed to the cathode of the cell. The liquid feed DMFC had methanol mass transport and carbon dioxide release problems. The significant amount of carbon dioxide generated and released from the anode slowed down the diffusion of liquid methanol to the anode catalyst layer. The use of a vapor feed eliminated these problems and resulted in a greater power density, 165 mW cm^{-2} for active vapor feeding compared to 122 mW cm^{-2} for liquid feeding. Scott et al. [5] discussed four factors that may have an influence on the inferior performance of liquid feed systems: mass transfer characteristics, the extent of methanol crossover, poor gas release from the anode surface and localized cooling on the anode catalyst for active systems.

Shukla et al. [6] built an active vapor feed DMFC which used a peristaltic pump to feed methanol solution to a vaporizer. The vaporizer was heated to 200 °C and the resulting vapors were then introduced to the anode of the cell while pressurized oxygen was fed to the cathode of the cell. Using a 1% methanol solution, power densities of 41.25 mW cm^{-2} at 75 mA cm^{-2} were achieved with a fuel utilization of 0.56. Hogarth et al. [7] modified Shukla's et al. [6] electrode configuration and used low catalyst loadings in conjunction with a vapor feed system. A platinum loading of 2 mg cm^{-2} was used on the anode and 0.5 mg cm^{-2} was used on the cathode. Pressurized nitrogen was mixed with the vapors and transported the resulting mixture to the anode of the cell. Using oxygen and air on the cathode side peak power densities of 350 mW cm^{-2} and 220 mW cm^{-2} were achieved, respectively.

Hirsch et al. [8,9] designed an active vapor feed system which uses a movable shutter, aperture or two corresponding perforated materials to control the feed of methanol. When the shutters are opened, methanol is free to transport to the methanol delivery

* Corresponding author. Tel.: +1 860 486 0419; fax: +1 860 486 0479.
E-mail address: faghri@engr.uconn.edu (A. Faghri).

0017-9310/$ - see front matter © 2009 Elsevier Ltd. All rights reserved.
doi:10.1016/j.ijheatmasstransfer.2009.03.007

film. The methanol delivery film is a material that effects a phase change in methanol from the liquid to gas phase. When in the gas phase it is then fed to the anode of the fuel cell. The system can control the methanol feed by adjusting the open area of the perforated material.

Yang and Huang [10] described an active local vapor fuel cell for alcohol fuels. The cells are stacked on top of each other, anode to cathode, and connected in series. Fuel (alcohol solution) is fed initially in a liquid state until it reaches the anode. There is a heating element located on the anode side of the cell to at least partially vaporize the fuel near the catalyst layer. The resulting vapor mixture is then ionized by the catalyst and produces protons that permeate through the membrane. This system allows for the cell to operate at a higher temperature which results in greater power density and energy efficiency.

The vapor feed systems discussed thus far are active systems which include pumps, humidifiers, vaporizers and compressed gases [11]. Passive systems achieve vapor feed operation with no moving parts and no external power input. There are several methods for vaporizing methanol passively, from direct heating to membranes that cause a phase change in methanol. There are very few groups however that are working on passive vapor feed systems.

HaeKyuong Kim [12,13] developed a semi-passive DMFC which is fueled by methanol vapor. Methanol is fed into porous foam by a syringe pump at a rate of 0.3 $cm^3\ h^{-1}$. Methanol is then vaporized through a layer of Nafion 112 and then diffuses through a water barrier layer and a buffer layer. The water barrier layer is a Teflon membrane which blocks water from entering the porous foam and the buffer layer is fired alumina. Water and methanol mix in the buffer layer and then diffuse to the anode where they react. This vapor feed system was able to reach a maximum power density of 36 mW cm^{-2} which was 12 mW cm^{-2} less than that of the liquid feed system. The reduction in power was determined to be caused by methanol vapor supply limit suggesting the need to improve the MEA design for better transfer of methanol. The vapor feed system was able to run for 360 h between 20 and 25 mW cm^{-2} with a 57% fuel efficiency and 0.145 Wh cm^{-3} energy density. The fuel efficiency was 70% higher than the liquid fuel efficiency, 38%, and the energy density was 1.5 times greater than liquid energy density, 0.095 Wh cm^{-3}.

Drake et al. [14] proposed a vapor feed system that uses a surface area enhanced planar vaporization membrane to separate a liquid fuel storage cartridge from the vapor chamber. As methanol passes through the membrane it will undergo a phase change from liquid to gas. The gas phase is then allowed to freely diffuse to the anode of the cell. They also describe a narrow opening for fuel delivery that can operate as a pinching mechanism which controls methanol feed rates to the phase change membrane.

Ren et al. [15] from MTI Micro also described a vapor feed system that uses a methanol delivery film. Liquid methanol is stored in a highly concentrated (80–90%) form and is separated from the vapor chamber by a fuel delivery barrier. The fuel delivery barrier is a thin polymeric film. This barrier also acts as a methanol delivery film by causing a phase change in methanol as it passes through the membrane. Methanol vapor in the anode chamber mixes with a small amount of liquid water and is then oxidized.

Guo and Cao [16] developed a passive fuel delivery system for a DMFC using a capillary pump. Methanol is stored in a reservoir and wicked to the anode of the cell where it mixes with water *in situ* during cell operation. The delivery system showed long-term reliability for over 250 h, keeping the concentration of methanol at the anode of the cell between 1.0 and 5.0 M. Guo and Faghri [17,18] made a complete passive thermal fluids management system for miniature DMFCs, which consisted of fuel delivery, water management and air management systems. Pure methanol was stored in porous media and was preferentially wicked through several layers of porous media to the anode of a DMFC. Methanol mixed with water in the water-storage layers, immediately adjacent to the anode of the cell, which provided the dilute methanol solution for the reaction. Jewett et al. [19] improved the water management system by adding additional cathode GDLs and using a variety of air filters to improve the air management system. A numerical simulation of the thermal fluids management system was also performed to study the effects of water and methanol transport in the passive fuel cell system [20,21].

Guo and Faghri [22] later expanded these concepts to make a new innovative vapor feed system. Pure methanol was wicked from a reservoir to an evaporation pad where heat is applied and the methanol was vaporized. The heat can come from a variety of sources such as electrical heating, catalyst burning and heat recovery from the cell or the device it is powering. The delivery system showed long-term stability for over 600 h using a catalytic burner.

This paper will focus on the vapor feed delivery of methanol and improvements to the existing design by Guo and Faghri [22]. Pure methanol will be stored in a reservoir and wicked to an evaporation pad. A thin film electric heater will be used to supply heat to the evaporation pad where methanol will be evaporated. A hydrophilic "buffer" layer will be added to the anode of the cell to promote water and methanol distribution as well as mixing of the fluids. Measurement of electrical parameters such as current, voltage, power, internal resistance and vapor chamber properties such as pressure, relative humidity and carbon dioxide concentration will be taken. The electrical performance of the cell will be found as well as conditions for stable operation for constant current loading. Carbon dioxide concentration, relative humidity, pressure and temperature of the cell and evaporation pad will be used to make recommendations for future system improvements concerning issues such as carbon dioxide release and heat recovery.

2. Experimental

The fabrication, experimental setup and testing procedures used in this study will be described in this section. The cells used were miniature passive DMFCs with an active area of 9 cm^2 with a membrane electrode assembly (MEA) and structure similar to the design by Guo and Faghri [23] and Faghri and Guo [24]. The additional heating power, power density of the cell, fuel efficiency and energy efficiency were examined.

2.1. Fabrication

The MEA was made by hot pressing the anode gas diffusion electrode (GDE), membrane and cathode GDE together. The membrane used was Nafion 117 and the gas diffusion electrodes (GDEs) were made up of an E-TEK A-11 ELAT/DMFC/Std-A gas diffusion layer (GDL) with a catalyst loading applied to them. The anode side had a 5 mg cm^{-2} loading of Pt:Ru and the cathode side had a 5 mg cm^{-2} loading of Pt. The three layers were hot pressed for 5 min at 130 °C under a 2000 lb load. After this was completed the layers were removed from the hot press and cooled while still under a load.

An additional hydrophilic-treated piece of carbon cloth was added to the anode side to act as a buffer layer. The untreated carbon cloth was submerged in a solution of 200 mL water, 100 g Nyacol and 3.0 g Triton X-100 in a beaker and placed in an ultrasonic bath for 10 min. After ultrasonic cleaning, the beaker was placed in a vacuum chamber at −30 in Hg for 20 min. The remaining carbon cloth was then calcined in air at 200 °C.

Two additional GDLs were added to the cathode side as water management layers as described in Jewett et al. [19]. The layers

were very thick – 480 μm – pieces of carbon cloth with a micro porous layer of 50% PTFE. These layers increased the hydraulic pressure at the cathode side of the cell and forced liquid water back through the membrane to the anode of the cell.

Platinum coated, niobium expanded metal mesh was used as the current collector on both sides of the MEA. The current collectors, additional layers and the MEA were held together using a fiberglass window frame structure with ribs. A vapor chamber is attached to the anode side of the cell and was sealed using a rubber gasket next to the frame and cover. An Oil Sorbents air filter was also applied to the cathode of the cell for protection, as well as further water and thermal management.

Water and methanol were stored externally in reservoirs for this prototype system to give more control over the system as well as to protect the cell and would not be needed for a real system. Water was wicked directly to the anode hydrophilic layer while methanol was wicked to the evaporation pad. The material for both wicks was a generic piece of cloth. The evaporation pad was Oil Sorbents material and was wrapped around the electrical heater and methanol wick. There was also a pinch valve located in the methanol wick that could be used to control the flow of methanol to the evaporation pad.

Methanol was evaporated using a thin film electric heater, which had a resistance of 14.4 Ohm and dimensions of 1 cm by 1 cm. The heater was placed inside the vapor chamber and the temperature of the heater was controlled by changing the voltage on the power supply. In the future, data taken during these tests will be used to design a heat recovery system so that the cell may eventually operate in a completely passive manner. A full schematic of the cell is shown in Fig. 1.

2.2. Experimental setup

Parameters that will be measured during testing include the electrical properties of the cell: resistance, voltage, current and power. This will be done using a Scribner Compact Fuel Cell Test Stand 850C which measures and records the fuel cell's performance. The temperature of the anode, cathode, evaporation pad and the ambient conditions will also be measured and recorded with K-type thermocouples using an Agilent 34970A data acquisition unit. The data acquisition unit also records the CO_2 concentration of the vapor chamber, which will be measured using a Vaisala 0–20% carbon dioxide probe. The relative humidity of the chamber as well as the pressure in the chamber will be measured and recorded using a Control Company humidity sensor 4189 and pressure meter 840065 with a 2 bar transducer.

2.3. Test procedures

The cell must first be activated after fabrication. This is accomplished by allowing it to soak in DI water for at least 2–4 h, after which the resistance of the cell should be stable while in water and less than 100 mOhm, preferably around 60 mOhm. Next 1.0 mol kg^{-1} methanol solution is added to the vapor chamber and the cell is run between 0.2 and 0.3 V for another 2–4 h. Once this is complete the cell is considered activated.

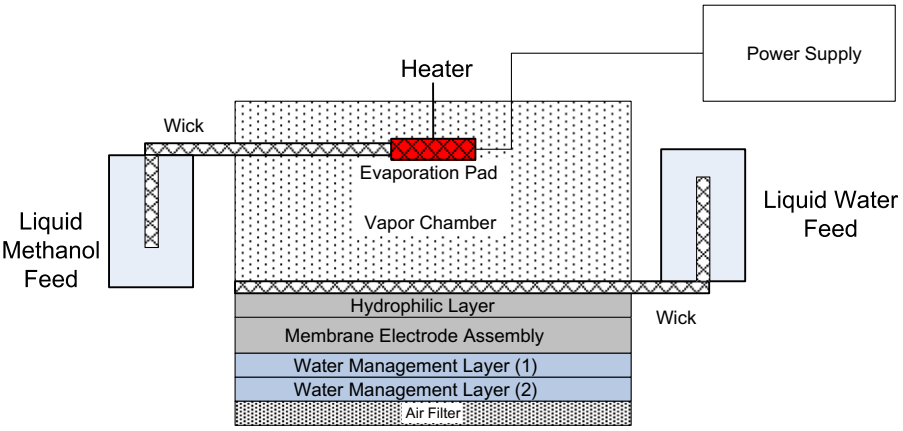

Fig. 1. Schematic of the passive vapor feed system for a DMFC.

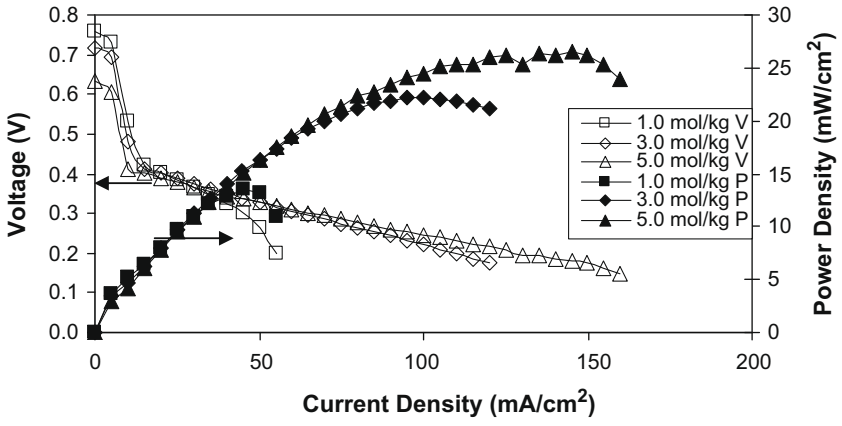

Fig. 2. DMFC#1 polarization curve of the cell with 1.0, 3.0 and 5.0 mol kg^{-1} concentrations in ambient conditions of 21 °C and 15% relative humidity.

Liquid polarization is performed next to confirm proper operation. Three methanol solutions of 1.0, 3.0 and 5.0 mol kg^{-1} are tested for polarization. The test consists of reading the voltage of the cell as the current density is changed. The current density begins at 0.0 mA cm^{-2} and is increased by 5 mA cm^{-2} until the cell voltage drops below 0.1 V. At each step the current density is held constant for 1 min and the average voltage is recorded.

Vapor feed testing consists of three tests: Startup, polarization and long-term constant current. The startup test consists of having the MEA of the cell thoroughly wet with water such that the resistance of the cell is as small as possible. The methanol wick and evaporation pad begin dry. Ten grams of methanol is added to the methanol reservoir and the open circuit voltage (OCV) of the cell is recorded. If heating is used it should be turned on before methanol starts wicking to the evaporation pad. The test is run until the cell's OCV reaches a maximum and then begins to decrease; this is the point at which the methanol has saturated the vapor chamber and has begun crossing over.

The vapor polarization test is conducted in the same manner as the liquid polarization test with the exception of the fuel delivery. Methanol is allowed to fully saturate the vapor chamber, as described in the cell startup, and the voltage is recorded as the current is scanned from 0 mA cm^{-2} and increased by increments of 5 mA cm^{-2} until the cell voltage drops below 0.1 V or the temperature exceeds 50 °C. The temperature and voltage limits are for protection of the cell.

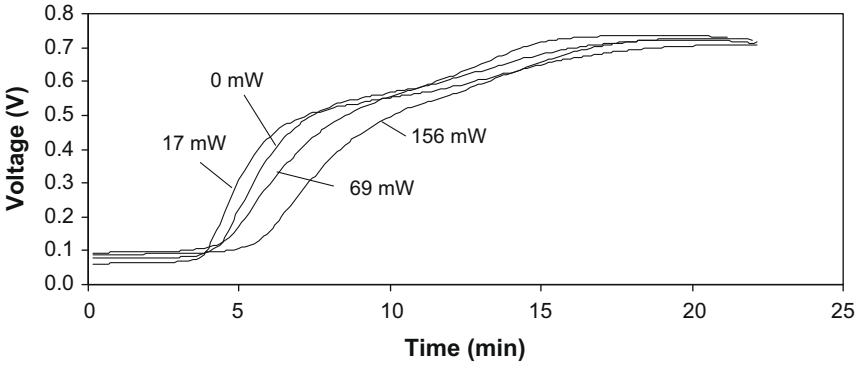

Fig. 3. DMFC#1 open circuit voltage during startup up of a vapor feed cell using four different heating powers.

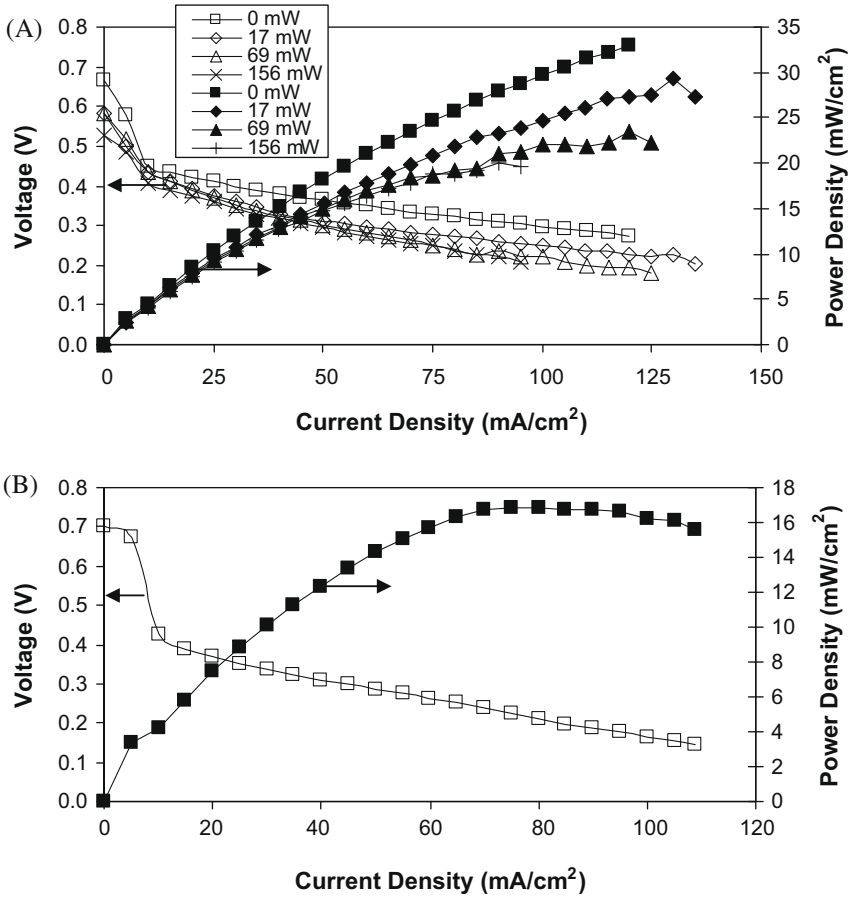

Fig. 4. DMFC#1 polarization curves for (A) vapor feed using different heating powers of 0, 17, 69 and 156 mW (B) 3.0 mol kg^{-1} liquid feed.

To test long-term, constant current the cell is run at 50 mA cm^{-2} and voltage of the cell is recorded. This is the maximum current density that can be used while keeping the cell temperature less than 50 °C. The amount of methanol and water consumed are recorded, as well as the temperature, pressure, relative humidity and carbon dioxide concentration.

Each vapor test is performed for a range of electrical heating, starting with no heating and increased until a stable setting is achieved. At this setting, the cell is run to observe the stability and efficiency of the vapor feed delivery system over a long period of time. Also, this provides information to improve the design with features such as carbon dioxide release and heat recovery.

3. Results and discussion

Two cells were built, DMFC#1 and DMFC#2 with the exact same MEA and additional layers. DMFC#1 was tested without any additional water on the anode at the start of tests and after a two week period the power density had decreased significantly. It is thought that anode catalyst contamination occurs due to ruthenium combining with oxygen from air in the anode GDE. DMFC#2 was built and tested with 1.0 g of water initially on the anode for all tests, which should force the majority of the air out of the anode and prevent or slow down the catalyst contamination.

After building the cells, they were activated using the procedure discussed in Section 2.3. After activation, the cell was kept in DI water so that the membrane was always hydrated when not in use. Liquid feed polarization was done first to ensure proper operation before vapor feed tests were started. Vapor feed polarization and long-term constant-current tests were then performed.

3.1. Performance characteristics of DMFC#1

The first step was to find the polarization curves for the cell using different concentrations. The current density was increased from zero, by increments of 5 mA cm^{-2} each step until the cell voltage dropped below 0.1 V. The polarization curves of the cell are shown in Fig. 2 for three methanol concentrations. When using a 1.0 mol kg^{-1} solution, the power density was low – less than 15 mW cm^{-2} – and the mass transfer limitation occurred very early at about 55 mA cm^{-2}. When the concentration was increased to 3.0 mol kg^{-1}, the maximum power density reached 22.5 mW cm^{-2} and the mass transfer limitation was increased to 120 mA cm^{-2}. Increasing the concentration to 5.0 mol kg^{-1} increased the maximum power density to 26.5 mW cm^{-2} and increased the methanol mass transport limitation to 160 mA cm^{-2}. The average temperature of the cell when using 5.0 mol kg^{-1} was significantly higher than other tests, 45 °C compared to about 27 °C, due to increased methanol crossover.

Now that the liquid feed performance had been verified, three aspects of methanol vapor feed delivery were examined, open circuit voltage (OCV) startup, polarization characteristics and long-term stability and performance.

The cell was started with the methanol wick dry. The anode of the cell was well hydrated and the internal resistance of the cell was less than 70 mOhms. The methanol reservoir was filled with 10 g of methanol before the wick was placed inside.

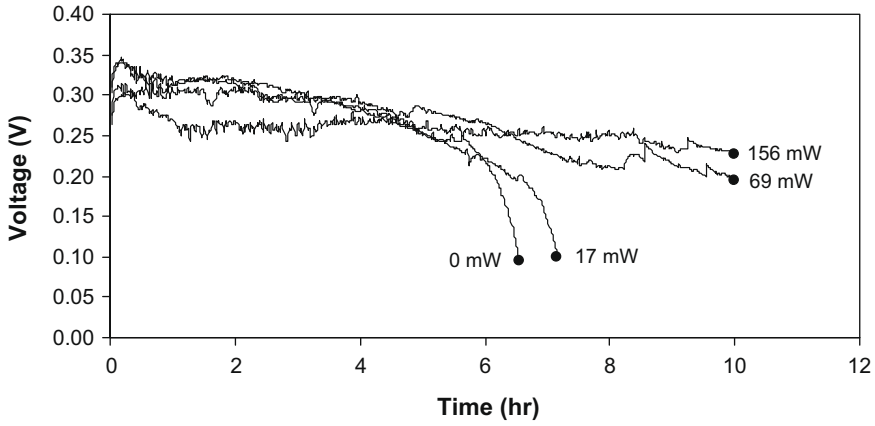

Fig. 5. DMFC#1 voltage over time under a constant current loading of 50 mA cm^{-2} for four different electrical heating inputs.

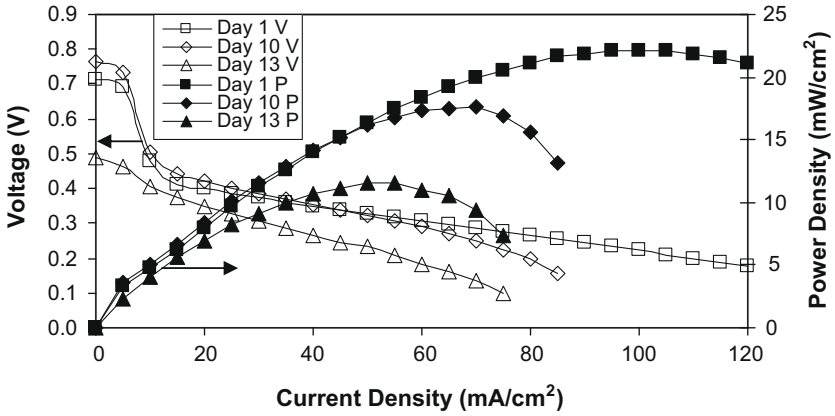

Fig. 6. DMFC#1 liquid polarization curves using 3.0 mol kg^{-1} solution over a span of 13 days. Ambient temperatures ranged from 20–26 °C.

The average amount of methanol needed to saturate the wick and bring the OCV to about 0.7 V was about 3.3 g. The OCV of the cell vs. time for each heating power is shown in Fig. 3. It took between 4 and 6 min for methanol to wick from the reservoir to the evaporation pad and begin to fill the chamber with vapor; this is the flat portion at the beginning of the test as shown in Fig. 3. As methanol filled the chamber and began to diffuse to the anode the OCV started to increase very rapidly to about 0.5 V. After the OCV reached 0.5 V, the production of methanol vapor began to increase the concentration at the anode and the OCV continued to rise, however much slower than the initial jump. When the chamber was fully saturated with methanol the OCV typically read about 0.7 V. As can be seen in Fig. 3, the amount of heating added to the evaporation pad had no trend on the startup of the cell from a dry state. Methanol is so volatile to begin with that it evaporated very quickly and did not need the extra heating during startup.

Once the cell reached a stable OCV after startup, the polarization of the cell was found. The results for the different heating powers are shown in Fig. 4A. When inspecting the results it would seem that increasing the heating reduced the performance. This is

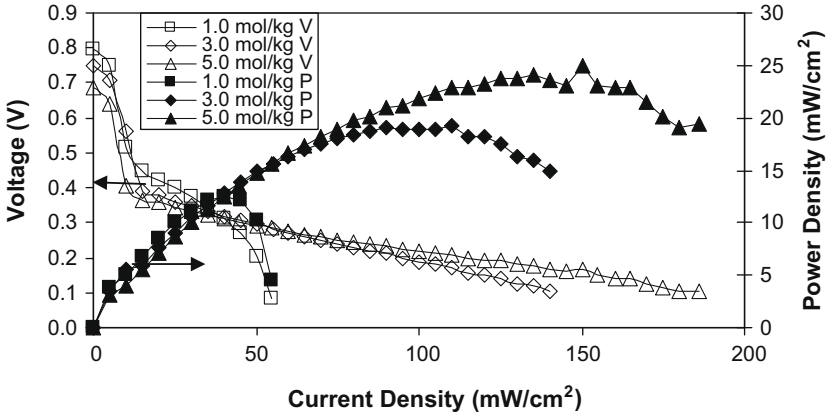

Fig. 7. DMFC#2 liquid polarization using 1.0, 3.0 and 5.0 mol kg^{-1} methanol solutions.

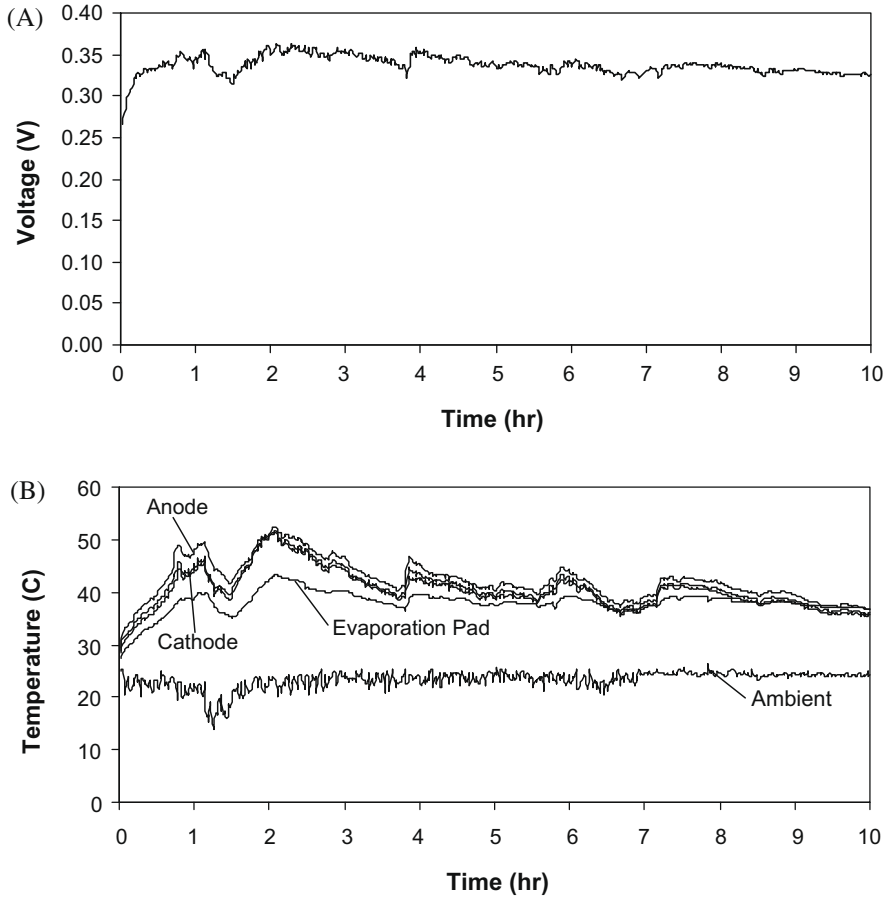

Fig. 8. DMFC#2 constant current, 50 mA cm^{-2}, 156 mW heating power, long-term (A) voltage and (B) temperature profile.

not necessarily the case, as some performance degradation occurred slowly during testing.

When comparing the vapor feed polarization to the liquid feed polarization it was found that even with no additional heating the cell achieved a much higher power density using the vapor feed system. The maximum power density achieved using 5.0 mol kg^{-1} solution was 26.5 mW cm^{-2} however the maximum power density reached using vapor feed delivery was 33 mW cm^{-2}, which may be even greater at higher current density.

Liquid feed polarization was performed again to check for performance loss; since the additional heating polarization decreased in power. Fig. 4B shows that the power density was about 5 mW cm^{-2} less than the original polarization test. This indicates that some performance losses occurred during the course of testing.

The cell was run in a constant-current mode of 50 mA cm^{-2} for 10 h or until the voltage of the cell dropped below 0.1 V. This was the highest current density that could be used while keeping the cell temperature less than 50 °C. Four different voltage inputs were used for the electrical heater, 0.0, 0.5, 1.0 and 1.5 V which correspond to heating powers of 0, 17, 69 and 156 mW.

The first issue that needs to be resolved for long-term testing is stability of the cell. This can be done by viewing the voltage profiles of the cells versus time during testing, Fig. 5. The natural evaporation case, 0 mW, had a stable voltage for only about 2 h, after which it decreased during the next 4 h to zero. Upon inspection of the cell, the evaporation pad and anode were still wet. The only possibility is that water from the anode evaporated and condensed on the evaporation pad. Water on the evaporation pad blocked the flow of methanol to the pad for evaporation and subsequently stopped the cell from producing power. This was solved by increasing the heating power of the pad such that condensation of water could be avoided.

As the heating power was increased the cells showed better stability with longer operational times. The 17 mW case was similar to the 0 mW case with a slightly longer operational time. The 69 mW case however, managed to maintain a cell voltage over 0.1 V for the full 10 h duration. A small decrease in cell voltage was observed and it was expected that the voltage would decay to 0.1 V after a long enough period of time. When the heating power was increased to 156 mW the cell showed good stability over the 10 h testing period with minimal decrease in cell voltage. The average cell voltage of the 156 mW heater power test was 0.257 V.

Another issue that occurred during testing was power degradation of the cell. The first liquid polarization curves using 3.0 mol kg^{-1} solution reached power densities over 20 mW cm^{-2}. During the 2 weeks of testing the cell, though, this power density decreased, Fig. 6. On day ten of testing, a liquid polarization test was performed to check cell performance. The maximum power density achieved with 3.0 mol kg^{-1} solution was 17.2 mW cm^{-2} compared to the initial 22.2 mW cm^{-2} power density of the cell. Three days later another liquid polarization test was done and the power density had decayed to a maximum of 11.6 mW cm^{-2}.

One possible cause of this power degradation is that the catalyst was deteriorating. On the anode side, it is possible for the ruthenium to combine with oxygen at high temperatures. During liquid feed testing this was not an issue because the liquid stored on the anode side would force the majority of oxygen out of the porous media. The liquid stored in the reservoir also provided a heat sink

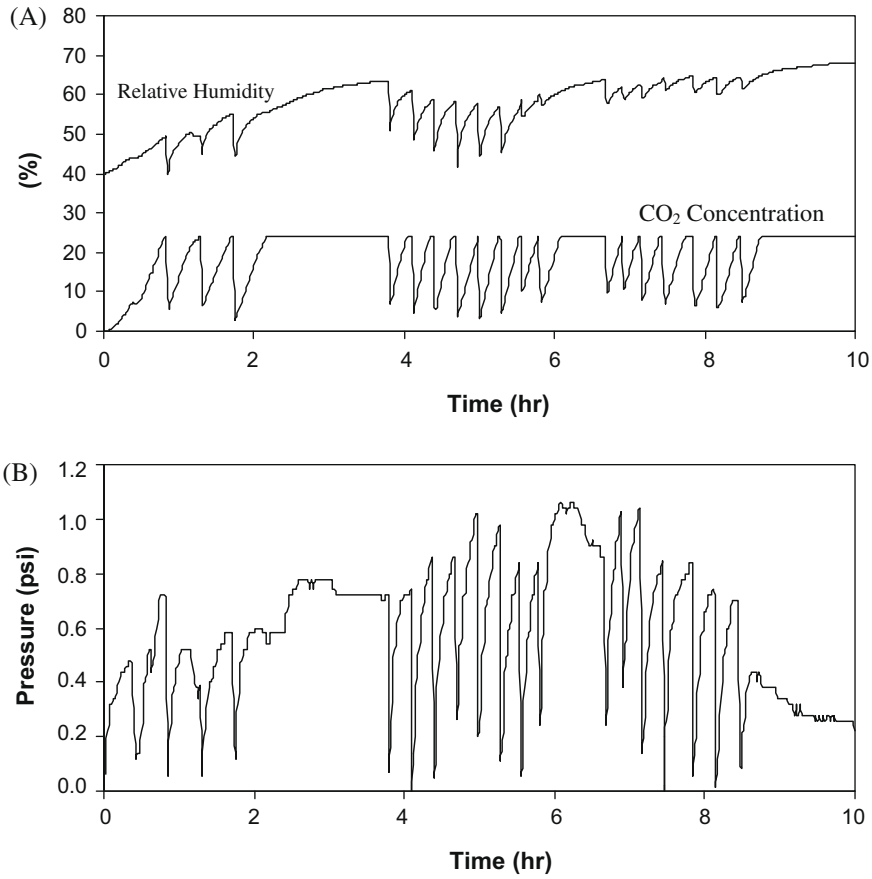

Fig. 9. DMFC#2 constant current, 50 mA cm^{-2}, 156 mW heating power, long-term (A) relative humidity, CO_2 concentration and (B) pressure in the vapor chamber.

for the cell during operation so that catalyst sites did not reach excessive temperatures. In the vapor feed system however, air is still present in the vapor chamber during testing and there is no liquid to act as a heat sink or to force oxygen out of the porous media.

3.2. Performance characteristics of DMFC#2

A second cell was fabricated in the exact same manner as DMFC#1. Liquid feed polarization testing was conducted to ensure proper operation of the cell, Fig. 7. DMFC#2 showed similar power density to DMFC#1 with a maximum power density of 25 mW cm^{-2} when using 5.0 mol kg^{-1}.

Long-term testing using a heater power of 156 mW and a constant current of 50 mA cm^{-2} was performed. The cell showed stable operation for 10 h with an average voltage of 0.337 V, Fig. 8A. The amount of solution depleted from the reservoir from start to finish was about 3.0 g. The fuel utilization efficiency determined for this test was 29.85% and the energy efficiency was 9.12%. The purging of CO_2 from the vapor chamber also evacuated some methanol from the chamber and is most likely responsible for the low efficiency.

The temperatures of the anode and cathode remained less than 50 °C while the room temperature stayed at an average of 23.3 °C, Fig 8B. The cathode temperatures were consistently 4–5 °C less than the anode temperatures. This is due to the cathode being cooled by the ambient environment while the anode is sealed off from the ambient conditions. The evaporation pad temperature was much less than the anode and cathode temperatures even though it was heated throughout the entire test. This was due to cooling effects from the evaporation of methanol from the pad. The evaporation pad also fluctuated similarly to the temperatures of the anode and cathode throughout testing.

The relative humidity in the chamber continuously increased in between vapor chamber purges, Fig. 9A. The initial relative humidity was 39.6% and the final relative humidity was 68.2%. This increase in relative humidity was caused by water evaporation from the anode of the cell where it was used to hydrate the membrane and also used in the anode reaction. This was also the primary reason for heating the evaporation pad. The water vapor in the chamber condensed on the evaporation pad because it had a lower temperature. Water condensation effectively blocked the flow of methanol to the evaporation pad and led to the cell ceasing operation. An increase in relative humidity is expected due to the constant feeding of water to the anode, water recovery and heating at the anode by the reaction.

The CO_2 concentration in the chamber increased very rapidly due to its formation at the anode from the methanol reaction, Fig. 9A. The concentration sensor could only read up to 24% concentration, therefore at this point the vapor chamber was purged by opening a hole and extracting some vapor using a syringe. This unfortunately extracted some of the methanol vapor in the process which lowered the efficiency of the cell. It is interesting to note that the profile of the pressure of the vapor chamber, Fig. 9B, matches the concentration profile. This suggests that the primary element that causes pressure in the vapor chamber is CO_2. A maximum pressure of about 1.0 psi was reached during a segment where CO_2 was not purged. Therefore, a method to release CO_2 is needed so that the primary component in the vapor chamber is methanol.

Using this information a micro check valve was obtained which opens at 0.04 psi. This should allow for CO_2 to escape without hav-

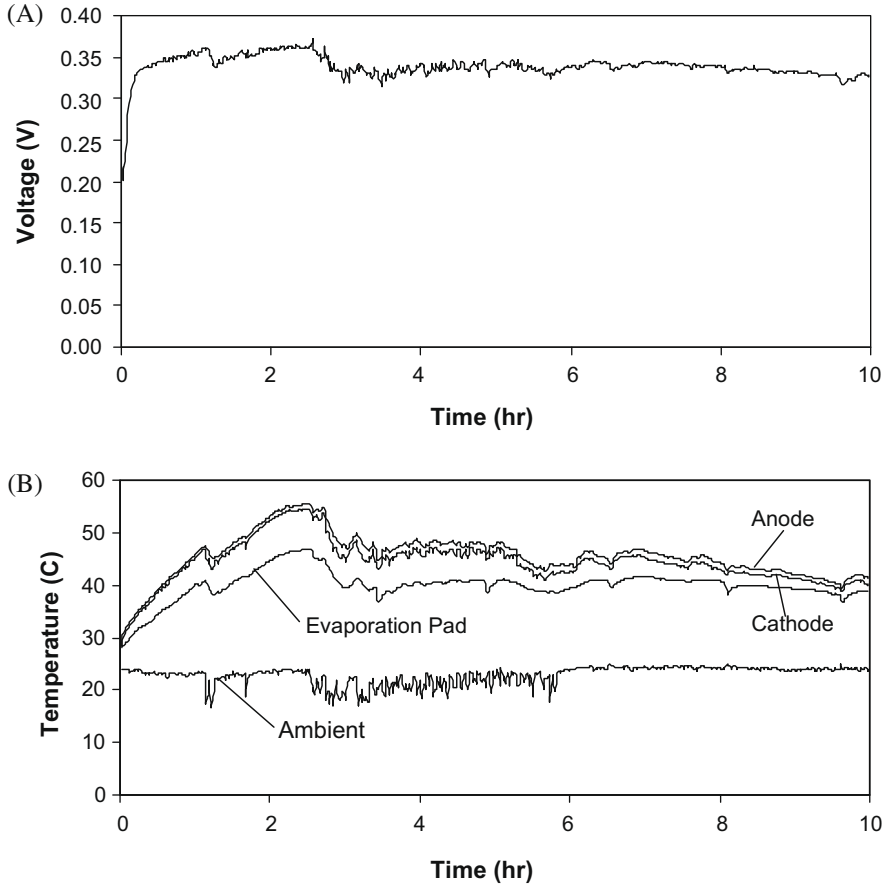

Fig. 10. DMFC#2 constant current, 50 mA cm^{-2}, 156 mW heating power, long-term (A) voltage and (B) temperature profile.

ing to purge the entire chamber, which should also reduce the amount of methanol vapor lost during operation. The check valve will also reduce the amount of air introduced into the chamber during operation. A preferable means of releasing CO_2 also includes a preferential membrane which allows CO_2 to escape but not methanol.

The cell was run at a constant current of 50 mA cm^{-2} for 10 h again with the micro check valve in the cover. The addition of the check valve had a negligible effect on the power of the cell; the cell voltage throughout the test was almost identical to the previous test, Fig 10A. The temperature profile also showed similar average readings as the previous test. The fuel utilization and energy efficiencies of the cell were slightly lower than the previous test, 27.8% and 8.5%, respectively. This was most likely due to methanol escaping through the check valve along with CO_2 when the valve was open. Again, a preferential membrane is needed to limit the amount of methanol lost through the valve.

The pressure of the cell stayed less than 0.06 psi during testing which shows that the check valve was working, Fig. 11A. The CO_2 concentration in the cell increased at a much slower rate and the vapor chamber only needed to be evacuated once every 1.5–2 h, Fig. 11B. This was significantly better than previous tests where the chamber needed to be purged every 30 min. The cell was purged by using a syringe to suck out the contents of the vapor chamber through the CO_2 and relative humidity sensor chamber. This resulted in an increase in the relative humidity during purging due to water from the anode being drawn out of the cell.

A third long-term constant current test was run on DMFC#2. The current was again set at 50 mA cm^{-2} and the cell was allowed to run for 5 days (120 h) uninterrupted with the exception of refueling the methanol and water reservoirs. The voltage and temperature profiles are shown in Fig. 12. Small changes in the voltage profile are related to changes in temperature of the cell and ambient conditions. The large decrease in voltage near the 50th hour is due to water flooding the anode. An excess amount of water was added to the cell because of high cell temperatures, which flooded the anode with too much water. This lowered the methanol concentration and the voltage of the cell.

The average room temperature was 22.9 °C over the 120 h duration. The temperatures of the cell and evaporation pad followed the normal trend with the anode of the cell having the greatest temperature. The cathode temperature was generally 3–4 °C less than the anode due to convective cooling to the ambient conditions. The evaporation pad was also lower than the anode temperature due to the evaporation of methanol.

The pressure of the chamber stayed below 0.06 psi due to the addition of the micro check valve from the previous test. This also kept the CO_2 concentration at a steady value of about 45%. The relative humidity slowly increased from 45% to 100% and remained at that value for the majority of the test. Between the relative humidity and resistance of the cell, which averaged about 40 mOhm, the hydration of the membrane can be ensured. If the membrane began drying out the relative humidity would begin to decrease and the resistance would increase. Neither of these conditions occurred which means that the membrane stayed hydrated throughout the test.

The total amount of water consumed and/or lost during the test was 16.65 g. The water balance coefficient was calculated and found to be about 1.04. This means that the cell was recovering about 1 molecule extra of water per molecule of methanol con-

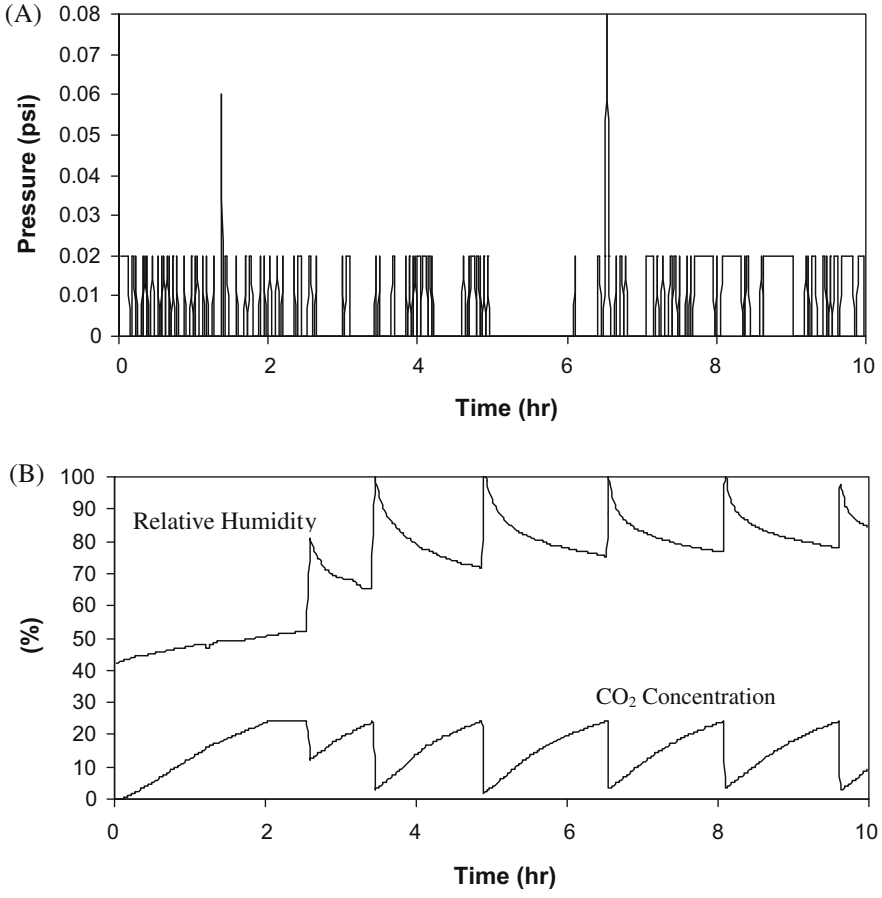

Fig. 11. DMFC#2 constant current, 50 mA cm^{-2}, 156 mW heating power, long-term (A) pressure (B) relative humidity and CO_2 concentration in the vapor chamber.

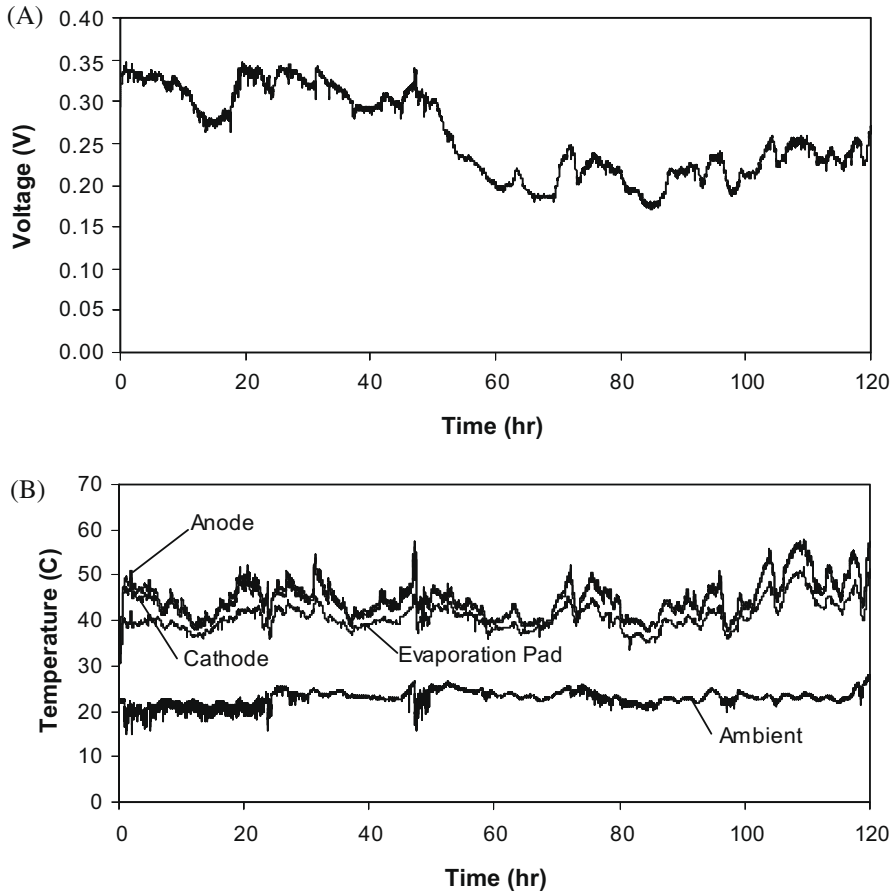

Fig. 12. DMFC#2 Constant current, 50 mA cm^{-2}, 156 mW heating power, long-term (A) voltage and (B) temperature profile.

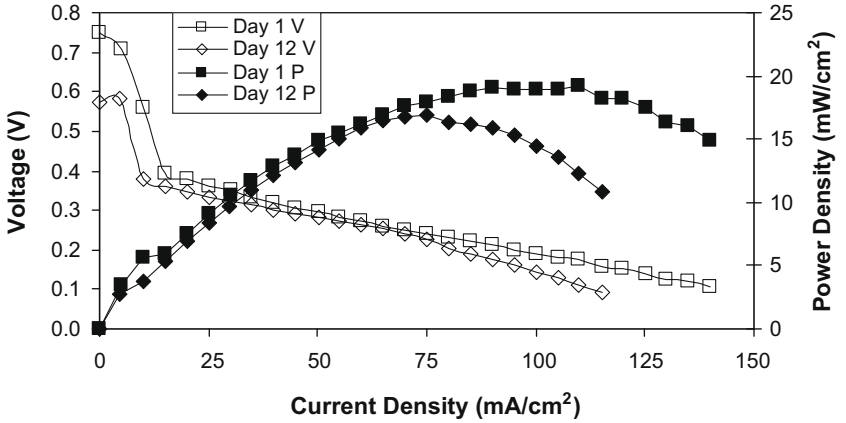

Fig. 13. DMFC#2 liquid polarization curves using 3.0 mol kg^{-1} solution over a span of 12 days. Ambient temperatures ranged from 20 to 25 °C.

sumed. Further improvements to the water management of the cell will be needed if it is to operate using pure methanol.

The total amount of methanol consumed during the 120 h duration was 30.82 g. The fuel utilization efficiency of the cell was calculated to be 34.8% and the energy efficiency was 8.2%. These are similar to the previous efficiency tests with the fuel utilization about 7% higher and the energy efficiency about 0.3% lower. The fuel utilization efficiency is greater when not purging the vapor chamber of CO_2 at any point during testing. This decreases the amount of methanol lost to the ambient room. The energy efficiency should also have increased, however, due to the lower voltage during the last half of the test, due to water flooding the anode, the net result was a slightly lower efficiency.

If the heating power of the electric heater is taken into account the energy efficiency will be even lower. The 14.4 ohm heater was run at 156 mW. Multiplying this number by the time that the test ran for, the resulting energy used by the heater was 67.5 kJ. This reduces the energy efficiency to −2.77%, meaning that more power was consumed than produced (50,436 J produced versus 67,500 J consumed). This demonstrates the need for some type of heat recovery device.

Reviewing the data, a simple conduction heating analysis can be performed using Fourier's Law $q = k\,\Delta T/x$. The heat flux was calcu-

lated to be 1562.5 Wm^{-2}. The average temperature difference between the anode and evaporation pad was about 4.4 °C. The distance between the anode surface and evaporation pad is about 1 cm. To transfer heat with these parameters, the thermal conductivity of the material would need to be 3.55 $Wm^{-1}\,K^{-1}$. Almost any metal will meet these requirements for simple conduction. There are also passive devices that are capable of transferring large amounts of heat passively, such as heat pipes and thermal spreaders, which should be considered. Further investigation into passive means of heat recovery and methanol evaporation is recommended.

Liquid polarization using a 3.0 mol kg^{-1} solution was performed again on DMFC#2 to see if there was any performance degradation, Fig. 13. The maximum power density achieved on the 1 day of testing was 19.2 mW cm^{-2} and a mass transport limitation of 140 mA cm^{-2}. Twelve days later the maximum power reached was 16.9 mW cm^{-2} and a mass transport limitation of 115 mA cm^{-2}. There is a 2.3 mW cm^{-2} reduction in power density and a 25 mA cm^{-2} reduction in mass transport limitation. Adding water to the anode at the beginning of tests seemed to have slowed down the performance decay of the cell. DMFC#1 had an 11 mW cm^{-2} decay after 13 days while DMFC#2 had only a 2.3 mW cm^{-2} decay after 12 days.

4. Conclusion

A vapor feed delivery system for a passive DMFC has been developed and tested. The vapor feed system is capable of achieving greater power density than a liquid feed system for the same cell, 33 mW cm^{-2} compared to 27 mW cm^{-2}. Measurements of the vapor chamber properties such as pressure, CO_2 and relative humidity were taken and improvements were made to the system. Constant current tests without heating the evaporation pad could not maintain a voltage over 0.1 V for more than 7 h, due to water condensing on the evaporation pad and blocking the flow of methanol. Long-term stability was achieved by using a thin film electric heater, at a power of 156 mW, to heat the evaporation pad. This vaporizes methanol as well as prevents water vapor from condensing on the pad. The release of the primary pressure component, carbon dioxide, was achieved by incorporating a micro check valve into the cover. The valve opens at very low pressure 0.04 psi which allows carbon dioxide to escape from the cell instead of building up. The vapor system was successfully operated for a 120 h (5 day) period. The fuel utilization efficiency during this period was 34.8% and the energy efficiency was 8.2%, not including the losses from the electrical heater.

Based on the information obtained from testing the two DMFCs a recommended system design can be determined. First, to ensure long-term reliability of the cell, sufficient water needs to be present at the anode at all times to force air out of the GDL as well as keeping the concentration around 2.0–3.0 mol kg^{-1}. The evaporation pad needs to be kept at a high enough temperature such that water cannot condense on the surface of the pad. The release of CO_2 from the vapor chamber will also release some water and methanol vapor, therefore a design which can preferentially release CO_2 and not methanol will increase the efficiency of the system. Development of a heat recovery system will also increase the efficiency of the cell and will allow the cell to run completely passively. To increase the cell's power density a cooling system may need to also be designed to keep the temperature of the cell below operational limits, 50–60 °C. The heat recovery and cooling system may be combined to achieve both tasks if designed properly.

References

[1] Z. Guo, A. Faghri, Challenges and opportunities of thermal management issues related to fuel cell technology and modeling, Int. J. Heat Mass Transfer 48 (2005) 3891–3920.
[2] B.K. Kho, B. Bae, M.A. Scibioh, J. Lee, H.Y. Ha, On the consequences of methanol crossover in passive air-breathing direct methanol fuel cells, J. Power Sour. 142 (2005) 50–55.
[3] J.G. Liu, T.S. Zhao, R. Chen, C.W. Wong, The effect of methanol concentration on the performance of a passive DMFC, Electrochem. Comm. 7 (2005) 288–294.
[4] E. Ralph, B.E. White, Conway, Mod. Aspect. Electrochem. 33 (1999) 104–107.
[5] K. Scott, W.M. Taama, P. Argyropoulos, Engineering aspects of the direct ethanol fuel cell system, J. Power Sour. 79 (1999) 43–59.
[6] A.K. Shukla, P.A. Christensen, A. Hamnett, M.P. Hogarth, A vapour feed direct-methanol fuel cell with proton-exchange membrane electrolyte, J. Power Sour. 55 (1995) 87–91.
[7] M. Hogarth, P. Christensen, A. Hamnett, A. Shukla, The design and construction of high-performance direct methanol fuel cells. 2. Vapour-feed systems, J. Power Sour. 69 (1997) 125–136.
[8] R.S. Hirsch, P.F. Mutolo, J.J. Becerra, R.K. Sievers, J.P. Scartozzi, W.P. Acker, Vapor feed fuel cell system with controllable fuel delivery, United States Patent 20040209133, 2004.
[9] R.S. Hirsch, P.F. Mutolo, J.J. Becerra, R.K. Sievers, J.P. Scartozzi, W.P. Acker, Vapor feed fuel cell system with controllable fuel delivery, United States Patent 20070026279, 2007.
[10] L. Yang, W.C. Huang, Local vapor fuel cell, United States Patent 20050164059, 2005.
[11] J. Kallo, W. Lehnert, R. von Helmolt, Conductance and methanol crossover investigation of nafion membranes in a vapor-fed DMFC, J. Electrochem. Soc. 150 (2003) A765–A769.
[12] Hae-Kyoung Kim, Passive direct methanol fuel cells fed with methanol vapor, J. Power Sour. 162 (2006) 1232–1235.
[13] Hae-Kyoung Kim, Jung-Min Oh, Jae-Yong Lee, H. Chang, Fuel cell system comprising vapor-phase fuel supplying system, United States Patent 20060269825, 2006.
[14] J.A. Drake, A.G. Gilicinski, G.G. Guay, L. Pinnell, Enhanced fuel delivery for direct methanol fuel cells, United States Patent 20050056641, 2005.
[15] X. Ren, J.J. Becerra, R.S. Hirsch, S. Gottesfeld, F.W. Kovacs, K.J. Shufon, Controlled direct liquid injection vapor feed for a DMFC, United States Patent 20050170224, 2005.
[16] Z. Guo, Y. Cao, A passive fuel delivery system for portable direct methanol fuel cells, J. Power Sour. 132 (2004) 86–91.
[17] Z. Guo, A. Faghri, Miniature DMFCs with passive thermal-fluids management system, J. Power Sour. 160 (2006) 1142–1155.
[18] Z. Guo, A. Faghri, Development of a 1W passive DMFC, Int. Commun. Heat Mass Transfer 35 (2008) 225–239.
[19] G. Jewett, Z. Guo, A. Faghri, Water and air management systems for a passive direct methanol fuel cell, J. Power Sour. 168 (2007) 434–446.
[20] J. Rice, A. Faghri, A. Transient, Multi-phase and multi-component model of a new passive DMFC, Int. J. Heat Mass Transfer 49 (2005) 4804–4820.
[21] J. Rice, A. Faghri, Thermal and startup characteristics of a miniature passive liquid feed DMFC system including continuous and discontinuous phase limitations, ASME J. Heat Transfer 130 (2008).
[22] Z. Guo, A. Faghri, Vapor feed direct methanol fuel cells with passive thermal-fluids management system, J. Power Sour. 167 (2007) 378–390.
[23] Z. Guo, A. Faghri, Development of planar air breathing direct methanol fuel cell stacks, J. Power Sour. 160 (2006) 1183–1194.
[24] A. Faghri, Z. Guo, Integration of heat pipe into fuel cell technology, Heat Transfer Eng. 29 (2008) 232–238.